JACS
JOURNAL OF THE AMERICAN CHEMICAL SOCIETY

Article

pubs.acs.org/JACS

Metal-Free on-Surface Photochemical Homocoupling of Terminal Alkynes

Luciano Colazzo,[*,†,‡] Francesco Sedona,[*,†] Alessandro Moretto,[†] Maurizio Casarin,[†,‡] and Mauro Sambi[†,§]

[†]Dipartimento di Scienze Chimiche, Università di Padova, Via Marzolo 1, 35131 Padova, Italy

[‡]CNR-ICMATE, Via Marzolo 1, 35131 Padova, Italy

[§]Consorzio INSTM, Unità di Ricerca di Padova, Via Marzolo 1, 35131 Padova, Italy

Supporting Information

ABSTRACT: On-surface synthesis involving the homocoupling of aryl-alkynes affords the buildup of bisacetylene derivatives directly at surfaces, which in turn may be further used as ingredients for the production of novel functional materials. Generally, homocoupling of terminal alkynes takes place by thermal activation of molecular precursors on metal surfaces. However, the interaction of alkynes with surface metal atoms often induces unwanted reaction pathways when thermal energy is provided to the system. In this contribution we report about light-induced metal-free homocoupling of terminal alkynes on highly oriented pyrolitic graphite (HOPG). The reaction occurred with high efficiency and selectivity within a self-assembled monolayer (SAM) of aryl-alkynes and led to the generation of large domains of ordered butadiynyl derivatives. Such a photochemical uncatalyzed pathway represents an original approach in the field of topological C−C coupling at the solid/liquid interface.

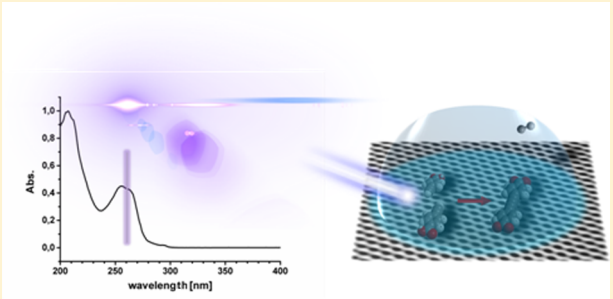

INTRODUCTION

On-surface coupling of simple molecular precursors has been widely exploited for the production of molecular superstructures with tunable electronic and mechanical properties.[1−4] Several chemical reactions have been tested on different surfaces, mostly metal substrates, that have shown catalytic activity for reactions that hardly take place in solution.[5,6] Ullman coupling of aryl-halides,[4,7] dehydration of boronic acid,[8] C−H bond activation processes,[9] and azyde-alkyne cycloaddition[10] are only a few examples of the extended literature on this matter.

Recently, on-surface terminal alkyne homocoupling, commonly (if somewhat improperly) referred to as Glaser coupling,[11,12] gained growing interest as a result of its exploitation to produce sp- and sp^2-hybridized nanomaterials.[13−15] Alkyne homocoupling is a well-known chemical reaction taking place both in solution, by metals-catalysis,[16−20] and on-surface. As far as the on-surface synthesis is concerned, it is well-known that this reaction occurs on low Miller index Cu,[21] Ag,[22] and Au[23] surfaces by providing heat to the organic monolayers. However, the strong adsorbate−substrate interaction often induces unwanted side-reactions (cyclotrimerizations,[23,24] generation of metal−organic species,[25] and oligomers cross-linking[26]), which accompany the homocoupling.[22] These side-reactions frequently inhibit the production of extended and regular nanostructures so that the real challenge still remains to take control of the many possible reaction pathways. Besides the use of templating substrates[27] or the adoption of steric hindering groups,[22] promising approaches to overcome this limit rely on nonthermal activation processes of supported alkynes. Gao et al.[28] reported the photochemical coupling of aryl-alkynes on Ag(111), aiming at their on-surface photopolymerization. However, after several hours of UV irradiation, they were able to produce only short oligomers; moreover, the high surface diffusion barrier for the heaviest oligomers hindered a favorable intermolecular orientation under UV exposure. Furthermore, the reaction proved to be fairly insensitive to different wavelengths, thus indicating a possible indirect, i.e. substrate-mediated, molecular excitation.[29−32] The interaction between the alkyne group and the metallic substrate[33,34] certainly provides a rationale for this finding. Nevertheless, the actual role played by the substrate, essential for the occurrence and propagation of the on-surface reaction, or able to stray the mechanism from a straightforward C−C coupling into a multistep reaction pathway, has never been tackled from an experimental point of view.

Here we show that the photochemical, metal-free homocoupling of terminal alkynes (Scheme 1) readily occurs on highly oriented pyrolytic graphite (HOPG) with high efficiency and selectivity within a self-assembled monolayer (SAM) of aryl-alkynes. The reaction takes place at the solid/liquid interface

Received: April 7, 2016
Published: July 20, 2016

DOI: 10.1021/jacs.6b03589
J. Am. Chem. Soc. 2016, 138, 10151−10156

Scheme 1. Schematic Representation of the on-Surface Photochemical Homocoupling

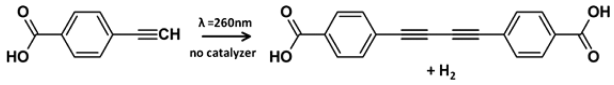

after short-time irradiation at the molecular precursor UV-resonant absorption wavelengths, eventually leading to the specific formation of butadiynyl derivatives.

Within the solid/liquid environment, the low activation barrier for the alkyne on-surface diffusion on the HOPG surface provides interfacial dynamics that possibly favors an appropriate intermolecular orientation upon the photon absorption event. In this view, the reduced or nearly absent photoconversion of the starting material with off-resonant wavelengths (irradiation wavelength out of the molecular UV-absorption band) ultimately testifies a direct molecular photoexcitation rather than a substrate-mediated mechanisms.[35,36] The experimental outcomes herein reported are consistent with a photoinduced topological C−C coupling at the solid/liquid interface. A single reaction product has been isolated and characterized in situ. The successful alkyne homocoupling reaction has been further confirmed by carrying out the same reaction ex-situ (in solution) and comparing the obtained products with the photochemically coupled precursors. Both the initial and the final molecular products and the ex-situ synthesized molecules were imaged by means of scanning tunneling microscopy (STM).

METHODS

In this study, the terminal alkyne of interest is a small π-system, namely 4-ethynylbenzoic (para-ethynylbenzoic) acid, hereafter called PEBA, purchased by Sigma-Aldrich and used without further purification. STM analysis at the solid/liquid interface has been carried out by preliminarily dissolving the reagent molecules in heptanoic acid (hereafter, 7COOH) at a concentration of 2.0 mg/g. A 5−15 μL droplet of solution was used for the observation of the interfacial behavior of the solute at the solid/liquid interface (see SI for further details).

Ex-situ synthesized molecules (4,4′-di(1,4-buta-1,3-diynyl)-benzoic acid (hereafter BUBA; see SI for the synthesis) where prepared for comparison with the photochemical reaction product and were analyzed under the same experimental conditions by using solutions at the same concentration.

Surface preparation was performed by scotch tape cleaving of the HOPG surface, and the surface cleaning was accurately checked prior to each deposition of the PEBA solution. Relatively clean and stable samples were obtained by drop-casting the solution at RT. Samples remained unaltered for several days, albeit, to limit contamination and solvent evaporation, STM investigations were performed just after the completion of the drop-casting process (see SI for further details). By using a tunable laser source we studied the behavior of our system at several wavelengths. The monochromatic light source used in this experiment was a tunable Nd:YAG laser system NT342A-SH (EKSPLA) equipped with an optical parametric oscillator (OPO). The output energy at the 260 nm wavelength was 1.71 mJ, pulse frequency 30 Hz, and pulse width 3.9 ns (see SI for further details).

RESULTS AND DISCUSSION

Drop-casting of a solution of PEBA in 7COOH on the HOPG surface produces a self-assembled and stable monolayer. Figure 1a shows a representative image of a 2D ordered aggregate of PEBA molecules. Islands, whose dimensions vary in the range 20−40 nm, are organized in symmetry-equivalent domains, according to the main directions of the underlying substrate

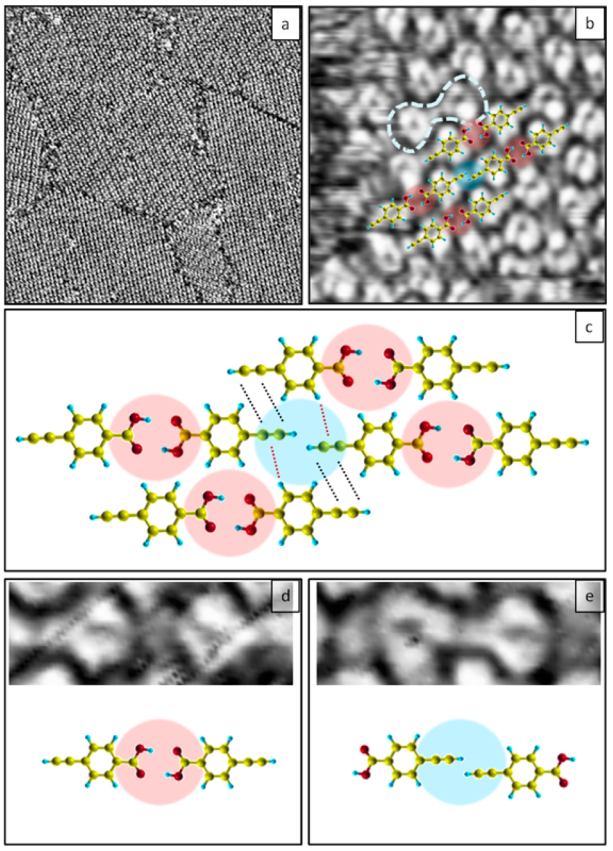

Figure 1. (a) Topographic (−0.70 V, 35 pA, 50 nm × 50 nm) and (b) high resolution STM image (−0.70 V, 35 pA, 5 nm × 5 nm) of the self-assembled structure of PEBA; (c) proposed ball and stick model of the PEBA supramolecular interaction network; (d) small-scale STM images of the carboxylic HB interaction and its corresponding proposed ball and stick model; (e) collinear alkyne interaction contrast feature and its corresponding proposed ball and stick model. See text for dashed and dotted lines and for red-/blue-shaded areas.

and show close-packed molecular building blocks. By high resolution STM imaging (Figure 1b), it is possible to observe that the superstructure is dominated by apparently dimeric species formed by two ring-like pairs interconnected by a bright feature, as outlined by the dashed line in Figure 1b. We propose that the observed dimers are composed of intact and flat-lying physisorbed PEBA molecules, with ring features corresponding to the benzene rings.[37] However, the labeling of the functional groups of the dimers remains not trivial.

PEBA molecules are heterofunctionalized with an ethynyl end-group and a carboxylic group pointing apart on a benzene ring (see superposition models in Figure 1b; shaded areas are a guide for the eye). Figure 1c (cf. shaded areas in Figure 1b) shows how the supramolecular order of PEBA molecules can be explained in terms of intermolecular hydrogen-bond (HB) networks. In more detail, two collinear hydrogen-bonded carboxylic groups (highlighted in red in Figure 1c) and their cooperative interactions with the nearest neighbor (NN) aromatic systems[38,39] provide a necessarily stabilizing interaction mesh. On the other hand, the collinear accommodation of the terminal alkynes (highlighted in blue in Figure 1c) is maintained by the stabilizing interaction of parallel alkyne groups involved in a 2-fold cyclic HB (C≡C−H···C≡C, see double-dotted lines in Figure 1c),[24,40] that sides with the

DOI: 10.1021/jacs.6b03589
J. Am. Chem. Soc. 2016, 138, 10151−10156

intermolecular interaction with their NN aromatic systems (dotted lines in Figure 1c).

According to recent investigations,[41,42] and in comparison with other reports of STM imaging regarding benzene-carboxylic acids,[43−46] the carboxylate groups appear darker with respect to the aromatic core for a combination of topographical and electronic effects around the negatively charged oxygens.[41] On this basis, we tentatively assign the dark area between the two rings to the HB between the collinear carboxylic groups (Figure 1d), while the aforementioned bright interconnection feature is ascribed to the alkyne end-groups approaching in a quasi-linear fashion, as depicted in Figure 1e.

In Figure 2a a high resolution image of ordered HB-dimers is shown: short black arrows, pointing toward the alkyne groups,

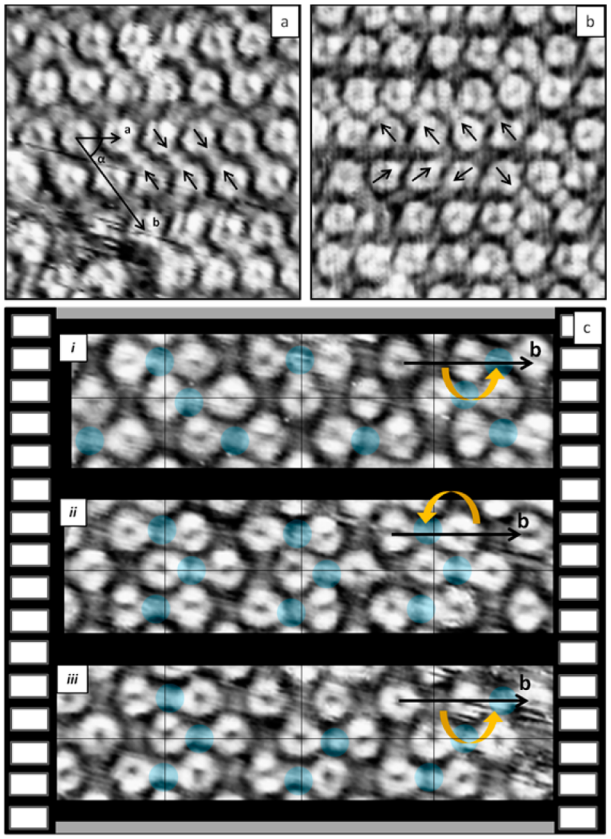

Figure 2. (a) STM image (−0.70 V, 25 pA, 5 nm × 5 nm) of an ordered aggregate of PEBA. (b) High resolution STM image (−0.40 V, 10 pA, 5 nm × 5 nm) of a disordered aggregate of PEBA. (c) Representative cartoon-clips for the observed on-surface dynamics over a selected area. Arrows and blue highlights are guides for the eye.

have been used to indicate molecular orientations. The ordered overlayer is reproduced by a unit-cell containing two molecules, whose parameters are a = 0.74 ± 0.05 nm, b = 1.89 ± 0.05 nm, and α = 55 ± 1°. These values have been obtained by averaging the real space measurements on five STM images, while, by high resolution imaging wherein both the substrate and the overlayer are present (SI, Figure S2a), the exact calibration of the molecular unit-cell based on the known size of the substrate lattice (0.264 nm) resulted in a = 0.74 nm, b = 1.86 nm, and α = 53° (see discussion in SI).

Along the overlayer vector b (see Figure 2a), a distance of 0.95 ± 0.05 nm is obtained as center-to-center distance for two phenyl rings interacting by carboxylic-HBs, while the distance between neighboring alkyne edges is 0.91 ± 0.05 nm. The former is consistent with the 0.96 ± 0.01 nm value found experimentally for the center-to-center distance between two NN terephtalic acid (TPA) molecules.[47] It is noteworthy that also vector a is reasonably consistent with the intermolecular distances found for TPA along the same packing direction (0.78 ± 0.01 nm). The NN alkyne−alkyne distance is also in reasonable agreement with the literature value of 0.80 ± 0.10 nm found experimentally for the 1,4-diethynylbenzene SAM on Cu.[24]

Alongside with the ordered 2D aggregates, also randomly oriented monomers have been observed (Figure 2b). These coexist in the PEBA SAM, where the aforementioned HB interaction network is involved in a dynamic-exchange equilibrium. Both tip-induced perturbations and the liquid environment can provide the driving forces for energetically accessible libration modes and discrete azimuthal rotations. These phenomena are reported in Figure 2c, as successive cartoon-clips (the alkyne end-groups have been highlighted in blue, and a grid has been added as a guide for the easy detection of the alkyne positions in different clips). Incidentally, also the complete rotation (two successive 180° on-site leaps) of a PEBA monomer has been detected (see yellow arrow in Figure 2c(i), (ii), (iii). Interestingly, if vector b is selected in the starting frame, its direction and length never change during the rotation of the central molecule (original images are in SI, Figure S3a, and a tentative modelization is in SI, Figure S3b).

Dynamic phenomena at the solid/liquid interface are generally associated with the vertical mobility of adsorbed molecules, as the supernatant liquid is responsible for a substantial lowering of the desorption barrier with respect to the vacuum barrier.[47] The on-surface dynamic processes observed within the PEBA superstructure imply that the underlying substrate does not strongly influence the aggregation pattern of the absorbed monolayer, although both adsorption/desorption processes and pattern rearrangements are energetically accessible at RT.

Crystalline PEBA reveals thermal and UV-induced reactivity. In the solid state, the photopolymerization reaction is topochemically promoted by the proximity of adjacent molecules within the crystal lattice.[48] We therefore assumed that by taking advantage of the collinear displacement of neighboring alkynes on the HOPG surface, a topochemical homocoupling could be promoted photochemically. According to the UV−vis spectrum of a solution of PEBA, the absorption band of the aromatic core is in the 240−270 nm range (see SI for further details). In order to maximize the photon absorption events, the 260 nm wavelength, which is a local maximum in the absorption curve, has been selected for irradiation. Direct exposure of the liquid cell to the laser beam for relatively short times (5−10 min) induced a nearly complete and irreversible conversion of the PEBA monolayer, resulting in a new molecular building block organized in a new ordered superstructure.

Figure 3a, b and insets report large and small scale images of the HOPG-supported monolayer before and after the light treatment. On the large scale it is evident that, after the illumination, the SAM is characterized by a new superstructure formed by ordered rows of dimeric species that organize in alternating, symmetrically equivalent domains.

After the UV irradiation, except for a few isolated unreacted monomers, almost all the molecular building blocks are constituted by dimers that, in contrast with the pristine HB-

DOI: 10.1021/jacs.6b03589
J. Am. Chem. Soc. 2016, 138, 10151−10156

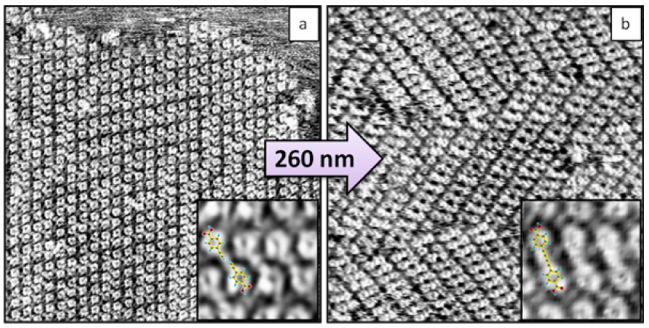

Figure 3. (a) Topographic STM image (−0.45 V, 10 pA, 20 nm × 20 nm) and (b) high resolution STM image (−0.30 V, 35 pA, 20 nm × 20 nm) after 5 min irradiation at 260 nm of the self-assembled PEBA superstructure. Insets are 2.5 nm × 2.5 nm close-ups of high resolution images obtained with similar tunneling conditions.

dimers, show no on-site rotations, suggesting the possible photoinduced stabilization of the molecular units with a chemical bond in the proposed butadiynyl derivative 4,4′-di(1,4-buta-1,3-diynyl)-benzoic acid, BUBA.

In the high resolution insets of Figure 3b it is also evident that the phenyl rings of BUBA are now connected by an intensified electronic density and the nodal plane observed in the pristine HB-dimers disappears. The center-to-center distance between the phenyl rings within an individual BUBA is 0.95 ± 0.05 nm, which is close to the distance found in the starting system, but nonetheless compatible with the 0.96 nm value obtained experimentally[12,28] and computationally[11] by other authors for various aryl-butadiynyl derivatives, and supports the occurrence of a photoinduced metal-free homocoupling reaction between terminal alkynes. The presence of a few unreacted PEBA monomers, constrained within ordered rows of the BUBA layer (see superposition models in Figure 4), allowed us to clearly compare the initial HB-interacting PEBA dimers with the photocoupled covalent dimers. The photocoupling involving the decarboxylation is

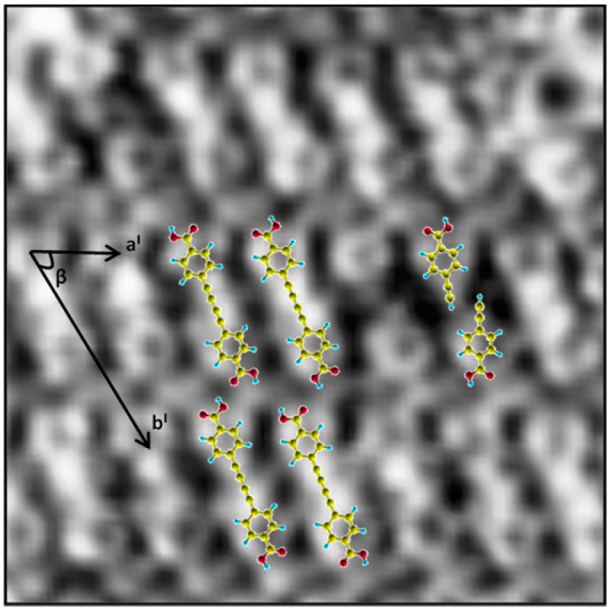

Figure 4. High resolution STM image (−0.30 V, 15 pA, 5 nm × 5 nm) of the photoreaction product and unreacted PEBA monomers.

unlikely to occur, since it would produce bis-phenyl species whose center-to-center distance is 0.43 nm, as found for oligo p-phenylene derivatives.[49,50]

The difference between the ordered SAMs before and after irradiation is more evident if one analyzes the corresponding unit-cells (exact calibration of the unit-cell in SI, Figure S2).

BUBA molecules have been observed to aggregate adopting specific schemes of carboxylic HB lateral interactions. Particular HB networks have been previously described[51] for this highly adaptable butadiynyl derivative. In our case, a bridging HB (representative unit-cell and molecular models are shown in Figure 4) has been observed. The superstructure is characterized by aggregates, whose arrangement is periodic and described by the unit-cell: $a^I = 0.68 \pm 0.05$ nm, $b^I = 1.71 \pm 0.05$ nm, and an angle $\beta = 65 \pm 1°$. For comparison, the exact and closest-commensurate unit-cell with the HOPG is $a^I = 0.65$ nm, $b^I = 1.77$ nm, and $\beta = 65°$ (see SI for the unit-cell determination). If this phase is compared to the initial system (a = 0.70 ± 0.05 nm, b = 1.89 ± 0.05 nm, and $\alpha = 55 \pm 1°$), its orientation with respect to the underlying HOPG changes (see Figure S2) and the unit-cells become smaller, noticeably along the alkyne axis, compatible with a photoinduced hydrogen dissociation and C−C coupling.

Previous reports show that monomer solutions of aromatic acetylenes undergo UV-induced polymerization and coupling reactions that occur in low yield and with low specificity.[52] A test was performed in order to exclude the occurrence of the homocoupling reaction in solution (Figure S4). A solution of PEBA in 7COOH was irradiated ex-situ under the same control conditions. Afterward, the UV-irradiated solution was checked with the STM on a clean HOPG substrate. In this case mostly PEBA molecules were observed by STM and, in particular, dimers were nearly absent. To further support the hypothesis of the topochemical control of the homocoupling reaction, we performed another control experiment in which we deposited a solution of excess PEBA and 1,3,5-benzenetribenzoic acid (TMA) (molar ratio PEBA/TMA = 40/1) in 7COOH on HOPG (see SI for experimental details). In this system, the aforementioned preorganization of PEBA is missing, as this molecule is less competitive toward the adsorption with respect to the tricarboxylic species and the preferential formation of the well-known ordered TMA superstructure emerges.[53−56] As a matter of fact, PEBA molecules intercalated within the TMA porous network and also small isolated clusters of PEBA could be observed among the boundaries of the extended TMA superstructure. Within this system, PEBA is mostly confined in solution (see Figure S4). After the irradiation of this system at 260 nm for various time intervals, the coupling reaction was less effective and mostly unreacted PEBA molecules were observed at the interface. Dimers conversion was estimated to be less than 10%. Noteworthy, photoinduced degradation of the TMA monolayer occurred. TMA has a nonzero absorbance at 260 nm,[57] and its superstructure degradation presumably occurs by dissipating the absorbed energy. In conclusion, the coupling reaction occurred far less efficiently within an irradiated solution where the proper topological preorganization of the monomers was missing or otherwise compromised, as when PEBA molecules are coadsorbed within the TMA lattice.

Other tests were also performed with 220, 240, 280, and 300 nm on the preformed PEBA SAM (see results in SI, Figure S6). Below 260 nm the system appeared disordered, presumably due to UV-induced degradation of both the organic solution and the overlayer. Above 260 nm the system was only partially

DOI: 10.1021/jacs.6b03589
J. Am. Chem. Soc. 2016, 138, 10151−10156

affected, and most starting material could be found unaltered. In conclusion, the reaction was less efficient in terms of sample quality and product yield over time at wavelengths far from the maximum of the absorption peak, indicating that a direct molecular excitation is needed for the coupling activation. Once the proper reaction conditions were established, the irradiation at 260 nm showed the highest rate and quality of product conversion with high reproducibility.

To further corroborate the successful photoinduced reaction, the bis-acetylenic dimer has been synthesized ex-situ with a Cu-catalyzed solution-reaction (see synthesis in the SI). Synthetic dimers have been dissolved in 7COOH and deposited on the HOPG surface. By STM imaging under the same conditions, we observed that the synthetic products aggregate in islands whose dimensions were measured in the range 20−50 nm (Figure 5a). By high resolution imaging (Figure 5b), unit-cell

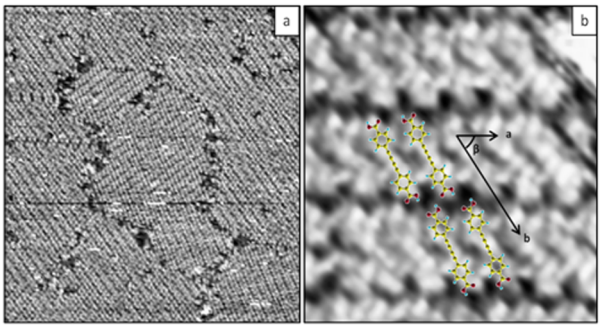

Figure 5. (a) Topographic STM image (−1.10 V, 5 pA, 50 nm × 50 nm) of the self-assembled structure of the ex situ synthesized bis-acetylenic dimer. (b) High resolution STM image (−0.50 V, 25 pA, 5 nm × 5 nm) of the self-assembled structure of the ex situ synthesized PEBA dimer.

parameters could be obtained by averaging real-space measurements on five images. Vectors a = 0.67 ± 0.05 nm, b = 1.78 ± 0.05 nm, and β = 63 ± 2° resulted similar to the BUBA SAM obtained in situ. Finally, the wet-reaction product clearly showed the same STM contrast at the molecular level, resulting from a similar carboxylic-HB bridging phase, as was found for the photochemically coupled PEBA products.

CONCLUSION

In this work we demonstrate that metal-free photochemical homocoupling occurs between terminal alkynes at the HOPG/liquid interface. This is obtained within a PEBA monomer SAM by exploiting its preorganization, i.e. the topological activation of the photochemical alkyne homocoupling. The successful C−C covalent stabilization is triggered by UV-light, it occurs catalyst-free, and the substrate acts only as a template, favoring the proper molecular orientation upon the photon absorption event. The comparison of the self-assembly patterns produced by in situ photoreacted monomers and ex-situ synthesized dimers allowed us to confirm the chemical nature of the photoreaction product. Also, the in situ photochemical conversion proved to be faster and cleaner with respect to the wet synthesis (5 min versus days and several purification steps, for a complete synthetic route) and the reaction selectivity showed up in monodispersity, which is noteworthy, given the many byproducts observed in the various metal-catalyzed Glaser couplings reported so far and referenced above.

The photoinduced mechanism occurred only with absorption-resonant irradiation, which in comparison with the metal-supported layers behavior[28] points toward a direct molecular excitation in accordance with a weak coupling with the underlying substrate. Photochemical activation on the weakly interacting HOPG thus proves to yield higher reaction selectivity when compared with thermal activation mechanisms observed on metal substrates, which induce disordered intermolecular interactions and broaden the product distribution.

The simple but heterofunctionalized starting material may eventually provide inspiration, biased by the recent debate on the on-surface reactivity of terminal alkynes, for the construction of more sophisticated superstructures by metal-free protocols and rational design of the molecular building blocks.

ASSOCIATED CONTENT

Supporting Information

The Supporting Information is available free of charge on the ACS Publications website at DOI: 10.1021/jacs.6b03589.

Detailed description of sample preparation and characterization (PDF)

AUTHOR INFORMATION

Corresponding Authors

*luciano.colazzo@studenti.unipd.it
*francesco.sedona@unipd.it

Notes

The authors declare no competing financial interest.

ACKNOWLEDGMENTS

This work was partially funded by MIUR (PRIN 2010/11, Project 2010BNZ3F2: "DESCARTES") and by the University of Padova (Grant CPDA154322, Project AMNES).

REFERENCES

(1) Nitzan, A.; Ratner, M. A. *Science* **2003**, *300* (5624), 1384.
(2) Wan, S.; Gándara, F.; Asano, A.; Furukawa, H.; Saeki, A.; Dey, S. K.; Liao, L.; Ambrogio, M. W.; Botros, Y. Y.; Duan, X.; Seki, S.; Stoddart, J. F.; Yaghi, O. M. *Chem. Mater.* **2011**, *23* (18), 4094.
(3) Côté, A. P.; Benin, A. I.; Ockwig, N. W.; O'Keeffe, M.; Matzger, A. J.; Yaghi, O. M. *Science* **2005**, *310* (5751), 1166.
(4) Basagni, A.; Sedona, F.; Pignedoli, C. A.; Cattelan, M.; Nicolas, L.; Casarin, M.; Sambi, M. *J. Am. Chem. Soc.* **2015**, *137* (5), 1802.
(5) Otero, G.; Biddau, G.; Sánchez-Sánchez, C.; Caillard, R.; López, M. F.; Rogero, C.; Palomares, F. J.; Cabello, N.; Basanta, M. A.; Ortega, J.; Méndez, J.; Echavarren, A. M.; Pérez, R.; Gómez-Lor, B.; Martín-Gago, J. A. *Nature* **2008**, *454* (7206), 865.
(6) Sun, Q.; Zhang, C.; Kong, H.; Tan, Q.; Xu, W. *Chem. Commun. (Cambridge, U. K.)* **2014**, *50* (80), 11825.
(7) Basagni, A.; Ferrighi, L.; Cattelan, M.; Nicolas, L.; Handrup, K.; Vaghi, L.; Papagni, A.; Sedona, F.; Valentin, C.; Di Agnoli, S.; Sambi, M. *Chem. Commun.* **2015**, *51* (63), 12593.
(8) Zwaneveld, N. A. A.; Pawlak, R.; Abel, M.; Catalin, D.; Gigmes, D.; Bertin, D.; Porte, L. *J. Am. Chem. Soc.* **2008**, *130* (21), 6678.
(9) Zhong, D.; Franke, J.-H.; Podiyanachari, S. K.; Blömker, T.; Zhang, H.; Kehr, G.; Erker, G.; Fuchs, H.; Chi, L. *Science* **2011**, *334* (6053), 213.
(10) Díaz Arado, O.; Mönig, H.; Wagner, H.; Franke, J. H.; Langewisch, G.; Held, P. A.; Studer, A.; Fuchs, H. *ACS Nano* **2013**, *7* (10), 8509.
(11) Zhang, Y.-Q.; Kepčija, N.; Kleinschrodt, M.; Diller, K.; Fischer, S.; Papageorgiou, A. C.; Allegretti, F.; Björk, J.; Klyatskaya, S.;

DOI: 10.1021/jacs.6b03589
J. Am. Chem. Soc. 2016, 138, 10151−10156

Klappenberger, F.; Ruben, M.; Barth, J. V. *Nat. Commun.* **2012**, *3*, 1286.
(12) Gao, H. Y.; Franke, J. H.; Wagner, H.; Zhong, D.; Held, P. A.; Studer, A.; Fuchs, H. *J. Phys. Chem. C* **2013**, *117* (36), 18595.
(13) Haley, M. M.; Brand, S. C.; Pak, J. J. *Angew. Chem., Int. Ed. Engl.* **1997**, *36* (8), 836.
(14) Baughman, R. H.; Eckhardt, H.; Kertesz, M. *J. Chem. Phys.* **1987**, *87* (11), 6687.
(15) Klappenberger, F.; Zhang, Y.-Q.; Björk, J.; Klyatskaya, S.; Ruben, M.; Barth, J. V. *Acc. Chem. Res.* **2015**, *48* (7), 2140.
(16) Hay, A. S. *J. Org. Chem.* **1962**, *27* (9), 3320.
(17) Mo, G.; Tian, Z.; Li, J.; Wen, G.; Yang, X. *Appl. Organomet. Chem.* **2015**, *29* (4), 231.
(18) Zhu, M.; Ning, M.; Fu, W.; Xu, C.; Zou, G. *Bull. Korean Chem. Soc.* **2012**, *33* (4), 1325.
(19) Chinchilla, R.; Nájera, C. *Chem. Rev.* **2014**, *114* (3), 1783.
(20) Zhang, X.; Liao, L.; Wang, S.; Hu, F.; Wang, C.; Zeng, Q. *Sci. Rep.* **2014**, *4*, 3899.
(21) Li, Q.; Owens, J. R.; Han, C.; Sumpter, B. G.; Lu, W.; Bernholc, J.; Meunier, V.; Maksymovych, P.; Fuentes-Cabrera, M.; Pan, M. *Sci. Rep.* **2013**, *3*, 2102.
(22) Gao, H.-Y.; Wagner, H.; Zhong, D.; Franke, J.-H.; Studer, A.; Fuchs, H. *Angew. Chem., Int. Ed.* **2013**, *52* (14), 4024.
(23) Liu, J.; Ruffieux, P.; Feng, X.; Müllen, K.; Fasel, R. *Chem. Commun. (Cambridge, U. K.)* **2014**, *50* (76), 11200.
(24) Eichhorn, J.; Heckl, W. M.; Lackinger, M. *Chem. Commun. (Cambridge, U. K.)* **2013**, *49* (28), 2900.
(25) Liu, J.; Chen, Q.; Xiao, L.; Shang, J.; Zhou, X.; Zhang, Y.; Wang, Y.; Shao, X.; Li, J.; Chen, W.; Xu, G. Q.; Tang, H.; Zhao, D.; Wu, K. *ACS Nano* **2015**, *9*, 6305.
(26) Cirera, B.; Zhang, Y.-Q.; Klyatskaya, S.; Ruben, M.; Klappenberger, F.; Barth, J. V. *ChemCatChem* **2013**, *5* (11), 3281.
(27) Cirera, B.; Zhang, Y. Q.; Björk, J.; Klyatskaya, S.; Chen, Z.; Ruben, M.; Barth, J. V.; Klappenberger, F. *Nano Lett.* **2014**, *14* (4), 1891.
(28) Gao, H. Y.; Zhong, D.; Mönig, H.; Wagner, H.; Held, P. A.; Timmer, A.; Studer, A.; Fuchs, H. *J. Phys. Chem. C* **2014**, *118* (12), 6272.
(29) Tognolini, S.; Ponzoni, S.; Sedona, F.; Sambi, M.; Pagliara, S. *J. Phys. Chem. Lett.* **2015**, *6* (18), 3632.
(30) Hatch, S. R.; Zhu, X.-Y.; White, J. M.; Campion, A. *J. Chem. Phys.* **1990**, *92* (4), 2681.
(31) Gadzuk, J. W. *J. Chem. Phys.* **2012**, *137* (9), 091703.
(32) Zhu, X.-Y.; White, J. M. *J. Chem. Phys.* **1991**, *94* (2), 1555.
(33) Zhang, Y.-Q.; Björk, J.; Weber, P.; Hellwig, R.; Diller, K.; Papageorgiou, A. C.; Oh, S. C.; Fischer, S.; Allegretti, F.; Klyatskaya, S.; Ruben, M.; Barth, J. V.; Klappenberger, F. *J. Phys. Chem. C* **2015**, *119* (17), 9669.
(34) Björk, J.; Zhang, Y. Q.; Klappenberger, F.; Barth, J. V.; Stafström, S. *J. Phys. Chem. C* **2014**, *118* (6), 3181.
(35) Ishida, Y.; Togashi, T.; Yamamoto, K.; Tanaka, M.; Taniuchi, T.; Kiss, T.; Nakajima, M.; Suemoto, T.; Shin, S. *Sci. Rep.* **2011**, *1*, 64.
(36) Zhou, X.-L.; Zhu, X.-Y.; White, J. M. *Surf. Sci. Rep.* **1991**, *13* (3−6), 73.
(37) MacLeod, J. M.; Lipton-Duffin, J. A.; Cui, D.; De Feyter, S.; Rosei, F. *Langmuir* **2015**, *31* (25), 7016.
(38) Suzuki, H.; Yamada, T.; Kamikado, T.; Okuno, Y.; Mashiko, S. *J. Phys. Chem. B* **2005**, *109* (27), 13296.
(39) Arras, E.; Seitsonen, A. P.; Klappenberger, F.; Barth, J. V. *Phys. Chem. Chem. Phys.* **2012**, *14* (46), 15995.
(40) Steiner, T. *J. Chem. Soc., Perkin Trans. 2* **1995**, No. 7, 1315.
(41) Guo, X.; Marrucci, F.; Price, N.; Stewart, E. L.; Baum, J. C.; Olson, J. A. *J. Phys. Chem. C* **2015**, *119* (44), 24804.
(42) Tan, Q.; Sun, Q.; Cai, L.; Wang, J.; Ding, Y. *J. Phys. Chem. C* **2015**, *119* (23), 12935.
(43) Lackinger, M.; Griessl, S.; Markert, T.; Jamitzky, F.; Heckl, W. M. *J. Phys. Chem. B* **2004**, *108* (36), 13652.
(44) De Feyter, S.; De Schryver, F. C. *J. Phys. Chem. B* **2005**, *109* (10), 4290.
(45) Addou, R.; Batzill, M. *Langmuir* **2013**, *29* (21), 6354.
(46) Florio, G. M.; Stiso, K. A.; Campanelli, J. S. *J. Phys. Chem. C* **2012**, *116* (34), 18160.
(47) Song, W.; Martsinovich, N.; Heckl, W. M.; Lackinger, M. *J. Am. Chem. Soc.* **2013**, *135* (39), 14854.
(48) Njus, J. M.; Sandman, D. J.; Yang, L.; Foxman, B. M. *Macromolecules* **2005**, *38* (18), 7645.
(49) Lipton-Duffin, J. A.; Ivasenko, O.; Perepichka, D. F.; Rosei, F. *Small* **2009**, *5* (5), 592.
(50) Baker, K. N.; Fratini, A. V.; Resch, T.; Knachel, H. C.; Adams, W. W.; Socci, E. P.; Farmer, B. L. *Polymer* **1993**, *34* (8), 1571.
(51) Kley, C. S.; Čechal, J.; Kumagai, T.; Schramm, F.; Ruben, M.; Stepanow, S.; Kern, K. *J. Am. Chem. Soc.* **2012**, *134* (14), 6072.
(52) Rohde, O.; Wegner, G. *Makromol. Chem.* **1978**, *179* (8), 2013.
(53) Lackinger, M.; Griessl, S.; Heckl, W. M.; Hietschold, M.; Flynn, G. W. *Langmuir* **2005**, *21* (11), 4984.
(54) Griessl, S. J. H.; Lackinger, M.; Jamitzky, F.; Markert, T.; Hietschold, M.; Heckl, W. M. *J. Phys. Chem. B* **2004**, *108* (31), 11556.
(55) MacLeod, J. M.; Lipton-Duffin, J. A.; Cui, D.; De Feyter, S.; Rosei, F. *Langmuir* **2015**, *31* (25), 7016.
(56) Kampschulte, L.; Lackinger, M.; Maier, A.-K.; Kishore, R. S. K.; Griessl, S.; Schmittel, M.; Heckl, W. M. *J. Phys. Chem. B* **2006**, *110* (22), 10829.
(57) Lawrence, F. A. *Anal. Chem.* **1951**, *23* (12), 1882.

DOI: 10.1021/jacs.6b03589
J. Am. Chem. Soc. 2016, 138, 10151−10156